Synthesis, Characterization, and Antimicrobial Activity of Salisaldehyde-Based Terpolymeric Ligand and Its Transition Metal Complexes

SAAD M. ALSHEHRI, AMAL AL-FAWAZ, FADIA AL-GHAMDI, TANSIR AHAMAD

Department of Chemistry, King Saud University, Riyadh, Kingdom of Saudi Arabia

Correspondence to: Tansir Ahamad; e-mail: tahamed@ksu.edu.sa; Saad M. Alshehri; email: alshehri@ksu.edu.sa.

Received: May 27, 2015
Accepted: February 11, 2016

ABSTRACT: In this study, we first synthesized a salisaldehyde-based terpolymer (SBT) ligand using salisaldehyde and phenylthiourea with glutaraldehyde. We then synthesized SBT metal complexes (SBT-M(II)) with the use of transition metal ions, such as Co(II), Ni(II), Cu(II), and Zn(II). To elucidate the structure and geometry of the metal ions, SBT and SBT-M(II) were characterized by elemental and spectral analysis. SBT-Co(II) and SBT-Ni(II) showed six coordination bonds with two water molecules, whereas SBT-Cu(II) and SBT-Zn(II) showed four coordination bonds. Gel permeation chromatography was used to determine the molecular weight of SBT. The thermal stability of SBT and SBT-M(II) was tested using thermogravimetric and differential thermal analysis. Thermal kinetic parameters such as activation energy and exponential factor were calculated using the Coats–Redfern method. In addition, antibacterial activity of SBT and SBT-M(II) was evaluated against several bacterial and fungal cultures using the agar well diffusion method. The polarity of the metal ion in SBT-M(II) was reduced which might contribute to its superior antimicrobial property. Adv Polym Technol 2016, 00, 21689; View this article online at wileyonlinelibrary.com. DOI 10.1002/adv.21689

KEY WORDS: Activation energy, FT-IR, NMR, gel permeation chromatography (GPC), metal-polymer complexes

Introduction

In recent years, salisaldehyde-based terpolymers (SBTs) containing donor atoms such as nitrogen, sulfur, and oxygen have gained much attention in the field of polymer technology. SBTs provide an easy approach to synthesize polymers containing transition metal ions that can be used in various applications such as adhesives, coatings, packaging materials, and so on.[1,2] Such polymers containing metal ions are interesting and new class of materials that provide additional physical properties for both organic polymers as well as metal ions. Previously, several polymers and terpolymers and their metal complexes have been synthesized and have shown very promising antibacterial, antitumor, antiviral, antifungal, and drug delivery properties.[3–6] According to a previous study, polymer metal complexes showed superior biological activities when compared with their parental polymeric ligands owing to metal ions.[7] Since the past few decades, research on polymeric or terpolymeric ligands and their metal complexes has increased due to their potential application in various fields such as water treatment, controlled-drug release, and catalysis.[7–10] Furthermore, according to previous studies, several polymeric and terpolymeric ligands such as formaldehyde-based polymeric ligands and their metal complexes have been synthesized that exhibited promising antimicrobial property and thermal stability.[11–15] As per our present knowledge and based on our literature survey, there is no work that reported on salisaldehyde-, glutaraldehyde-, and phenylthiourea-based terpolymeric ligand and its terpolymeric metal complexes. Therefore, in this study, we aimed to synthesize SBT and its metal complexes (SBT-M(II)) with Co(II), Ni(II), Cu(II), and Zn(II) metal ions. The synthesized compounds were characterized using spectral, magnetic, and thermal analysis. Furthermore, we also discuss the type of coordination of polymeric ligand and the geometry of the metal ions. Thermal stability of SBT and SBT-M(II) was studied by thermogravimetric analysis (TGA) and differential thermal analysis (DTA). Kinetic parameters such as activation energy (E), order of reaction (n), as well as thermodynamic parameters such as free energy and entropy were also calculated. In addition, the antibacterial activity was tested against the following bacteria: *Bacillus subtilis, Escherichia coli, Staphylococcus aureus, Salmonella typhi, Psuedomonas aeruginosa*. The following fungi were used to test antifungal activity: *Candida albicans, flavus, Aspergillus niger, Fusarium solani, Mucor indicus*.

Experimental

MATERIALS

Salisaldehyde, phenylthiourea, glutaraldehyde, sodium hydroxide (NaOH), and metal salts were purchased from Sigma

Aldrich (Gmbh Munich, Germany). All the solvents were purified by standard procedures before use. Tryptic soy agar (TSA) and tryptic soy broth (TSB) were purchased from Difco Laboratories (Michigan, USA), and the strains were stored in a deep freezer until use.

MEASUREMENTS

The elemental analyses of SBT and SBT-M(II) were performed on a Perkin Elmer model-2400 elemental analyzer. The percentage of metal ions was determined by complexometric titration.[16] The Fourier transform infrared (FTIR) spectra of SBT and SBT-M(II) were recorded on a spectrophotometer (Bruker Tensor-27) (Bruker Optics, Ettlingen, Germany) between the range of 4000 and 400 cm^{-1}. The electronic spectra (UV–visible) were recorded on a Shimadzu UV–Vis spectrophotometer (UV-1650 PC), and the magnetic susceptibility was measured on a Gouy (Kyoto, Japan) balance by using $Hg[Co(SCN)_4]$ as the calibrator. Proton and carbon-13 nuclear magnetic resonance spectra (^1H NMR and ^{13}C NMR) were recorded on a JEOL–GSX 400-MHz FT NMR spectrometer (Massachusetts, United States) using δ_6-dimethyl sulfoxide (DMSO) as the solvent and tetramethylsilane (TMS) as an internal standard. The electron spin resonance (ESR) spectrum of the SBT-Cu(II) was recorded at room temperature on a Varian 112 ESR spectrophotometer. SDT Q-600 (TA Instrument, New Castle, Delaware, USA) was used to measure the thermal stability of SBT and SBT-M(II) in the presence of nitrogen at a heating rate of 5, 10, 15, or 20°C min^{-1}. The average number (M_n) and average weight (M_w) of SBT were measured by gel permeation chromatography (GPC) (Polymer Laboratories GPC220, Santa Clara, California, USA) using tetrahydrofuran (THF) as a mobile phase.

SYNTHESIS

Synthesis of SBT

In a 250-mL round bottom flask, salisaldehyde (1.06 mL, 10 mmol) and phenylthiourea (1.52 g, 10 mmol) were dissolved using 30 mL of ethanol. Then to this solution, glutaraldehyde (1.5 mL, 0.2 mmol) was added and mixed. Subsequently, 0.1 M aqueous NaOH solution was added dropwise until the pH of the solution reached up to 8–9. The reaction mixture was then refluxed at 80°C with continuous stirring for 5 h. A rotary evaporator was used to remove the excess solvent under reduced pressure. A light yellow-colored viscous product was obtained that was washed with distilled water and methanol, respectively, and was vacuum dried at 60°C for 24 h to produce SBT powder with a 75% yield.

Synthesis of SBT-M(II)

In a 250-mL flask, SBT (4.10 g, 10 mmol) was dissolved using 50 mL of THF. The metal chloride (5 mmol) was dissolved in 30 mL of ethanol, and both the solutions were mixed and stirred at 70°C for 5 h. Then, the excess solvent was removed under reduced pressure using a rotary evaporator. After that, the reaction mixture was cooled and precipitated using a 75/25 (v/v) water/methanol mixture. The precipitated SBT-M(II) was filtered and then reprecipitated using dimethylformamide (DMF) into methanol. The obtained precipitate was dried in a vacuum oven at 60°C for 24 h with a 75–80% yield.

ANTIMICROBIAL ACTIVITY

Antibacterial Activity

The synthesized SBT and SBT-M(II) were screened against *B. subtilis*, *Staphylococcus aureus*, *E. coli*, *P. aeruginosa*, and *Salmonella typhi* for evaluating their antibacterial activities using the agar well diffusion method.[17] Briefly, the samples were prepared in DMSO at a concentration of 50 μg/mL. Bacterial strains were grown in a nutrient broth (Difco) before incubated on Mueller–Hinton agar for 24 h. A sterile steel borer was used to dig wells in the media, and then 0.1 mL of sample solution was introduced in their corresponding well. Subsequently, the petri dishes were incubated at 37°C for 24 h. DMSO was used as the negative control and kanamycin as the positive control. All the petri dishes were examined for their zone of inhibition, and the diameter of the zone of inhibition was measured in millimeters. Each experiment was repeated at least three times.

Antifungal Activity

The antifungal activity of SBT and SBT-M(II) was evaluated against various fungi, namely, *C. albicans*, *A. flavus*, *A. niger*, *F.* spp., and *M.* spp. by the agar well diffusion method as per the previous reported method.[5] DMSO was used as negative control, and miconazole was used as a positive control. The samples were prepared using DMSO as the solvent at a concentration of 100 μg/mL. Stock solutions of miconazole were prepared in distilled water. The fungal strains were prepared in malt extract broth (Difco). Wells were dug in the media contained in petri dishes with the help of a sterile steel borer into which 0.1 mL of sample was introduced in their corresponding well. The petri dishes were then incubated at 30°C and were examined for the zone of inhibition. The diameter of the zone of inhibition was measured in millimeters. Each experiment was repeated at least three times.

Results and Discussion

PHYSICOCHEMICAL AND ELEMENTAL ANALYSIS

The condensation reaction between phenylthiourea, salisaldehyde, and glutaraldehyde was carried out in a 250-mL round-bottomed flask. A light yellow viscous product (SBT) was obtained after the completion of the reaction (Scheme 1). SBT-M(II) were synthesized with corresponding metal ions with a significant yield (Scheme 2). However, SBT-M(II) were not soluble either in water or in common organic solvents but was soluble in DMF and DMSO. The percentage of elements in SBT and SBT-M(II) was determined using elemental analysis, and the percentage of metal ions was determined by complexometric titration. In SBT-M(II), the metal ions and the monomeric unit of terpolymeric ligand were present at the 1:2 molar ratio, respectively. The results of elemental analysis suggest coordination number of four for SBT-Zn(II) and SBT-Cu(II) and six for SBT-Co(II) and SBT-Ni(II) after coordination

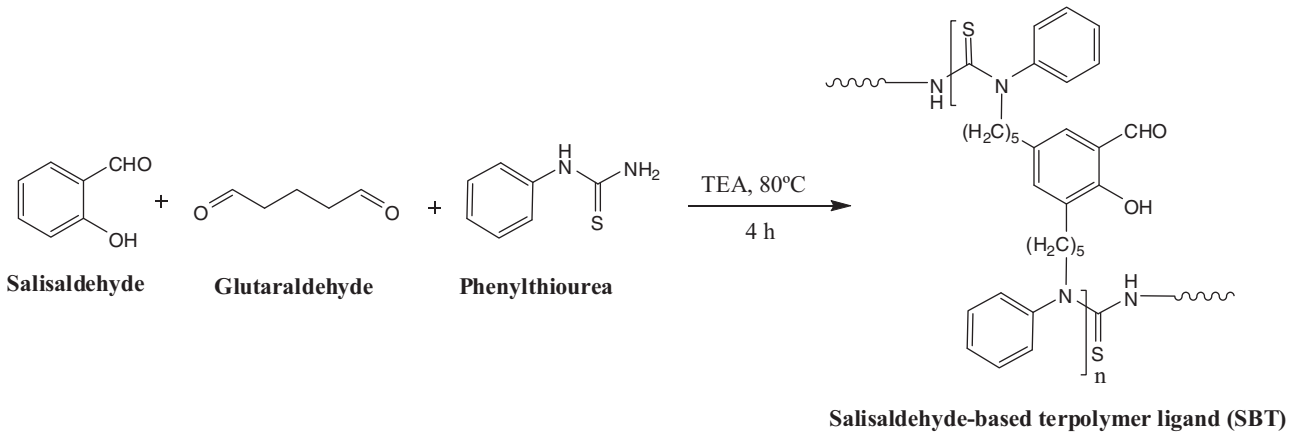

SCHEME 1.

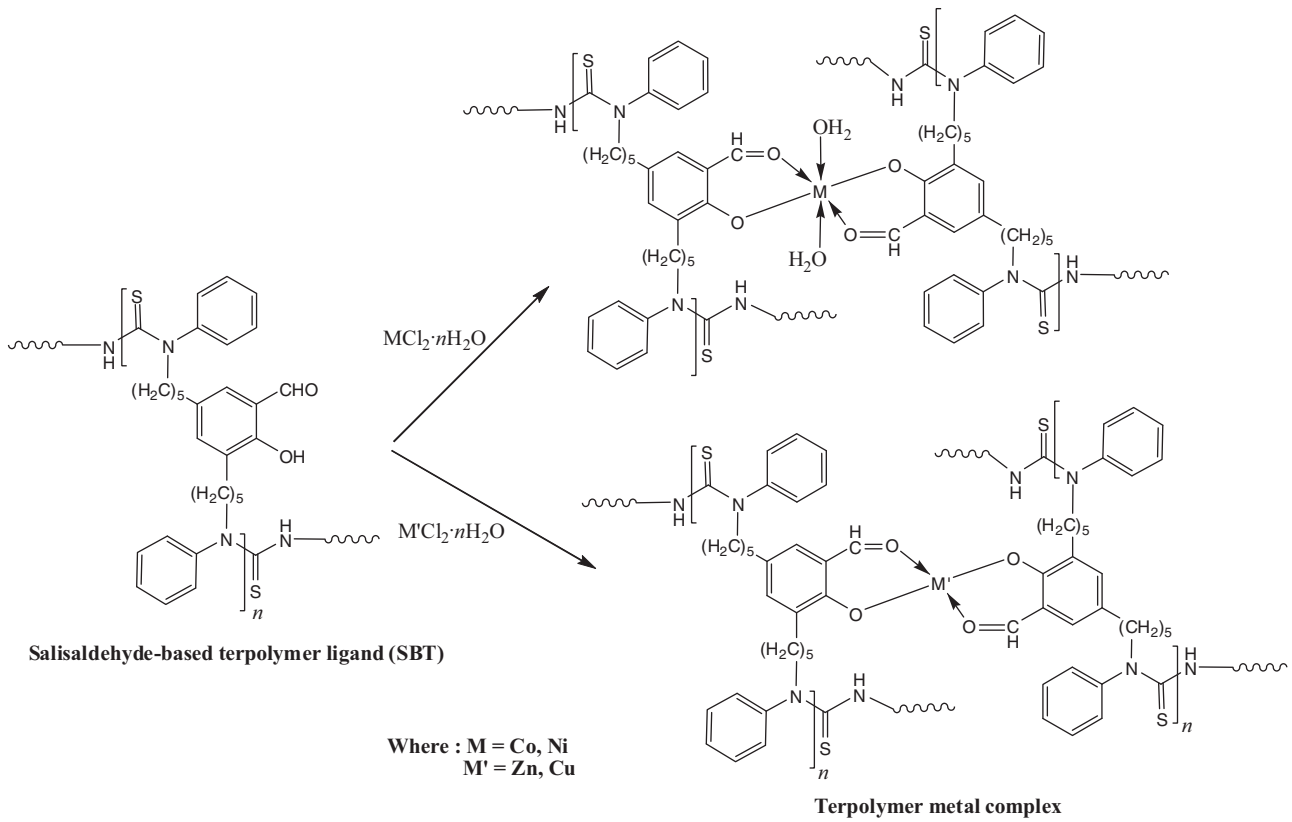

SCHEME 2.

with two water molecules. The molecular weight of SBT was carried out using GPC with THF as the standard. The weight average and number average molecular weight of SBT was found to be, respectively, 2168 and 2152 (Fig. 1). The polydispersity index (PDI) was found to be 1.0074. The results of GPC analysis clearly indicate that SBT has a narrow range distribution of molecular weight.[18] Owing to the insolubility of the metal complexes in THF, the molecular weight of SBT-M(II) could not be determined using GPC. Table I summarizes the results of elemental analysis including the color of synthesized compounds.

FTIR SPECTRAL ANALYSIS

Figure 2 illustrates the FTIR spectra of SBT and SBT-M(II). In case of SBT, a broad band in the range of 3556–3418 cm^{-1} is assigned to the stretching mode of the –OH group.[19] Another broad band due to the asymmetric and symmetric bending of νN–H was observed between 3281 and 3178 cm^{-1} regions. This bending may be due to the intermolecular hydrogen bonding[20] between sulfur or oxygen of thionyl and carbonyl groups with the hydrogen of the phenolic and amide groups. Another band appearing at 3071 and 1560 cm^{-1} correspond to the C–H stretching

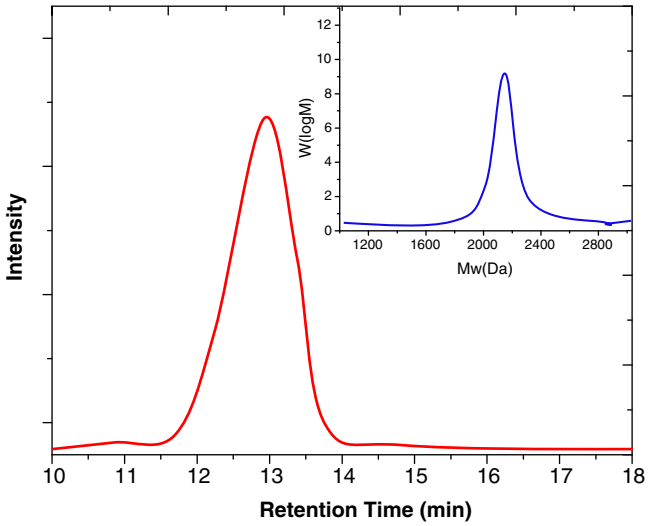

FIGURE 1. GPC plot of terpolymeric ligand (SBT).

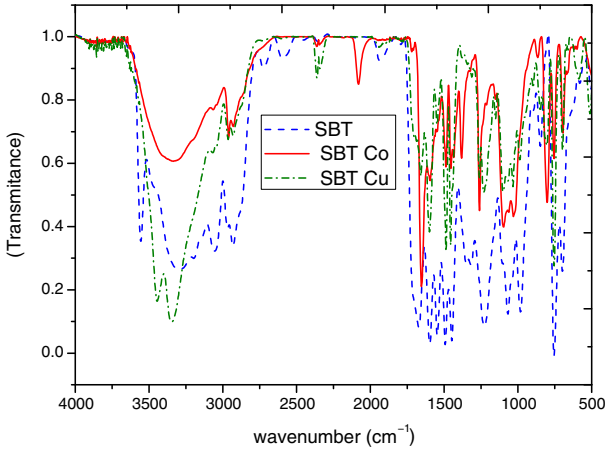

FIGURE 2. FTIR spectra of SBT ligand and its polymer metal complexes.

and C–H bending of the aromatic ring, respectively. Two strong FTIR bands between 2941 and 2871 cm^{-1} and between 1491 and 1450 cm^{-1} are attributed to the asymmetric and symmetric stretching and bending of the methylene group (νCH_2), which was formed during the condensation reaction with glutaraldehyde. The stretching frequency of the thionyl group (C=S) in SBT and SBT-M(II) is seen in the region of 1672 cm^{-1}. The stretching of carbonyl (C=O) group appears between 1650 and 1712 cm^{-1} region, which becomes broader; however, in case of SBT-M(II), a major shift toward lower wavenumber of 25–20 cm^{-1} has been found (1650–1685 cm^{-1}), which supports its coordination with the metal ions.[21] In the FTIR spectrum of SBT-M(II), the bands at 3550 cm^{-1} region become more broader due to the coordination of water molecules and the formation of metal–oxygen bonds.[22] The appearance of FTIR bands between 1614 and 1580 cm^{-1} region supports the presence of coordination water molecules in the FTIR spectra of SBT-Co(II) and SBT-Ni(II). Another band between 693 and 650 cm^{-1} is attributed to the rocking mode of coordination of water molecules. The FTIR bands belonging to the coordination of water molecules were not detected in the spectra of SBT-Cu(II) and SBT-Zn(II), which supports that SBT-M(II) have four coordination number complexes. Another FTIR band between 1382 and 1261 cm^{-1} is attributed to the stretching of the C–N bond of the coordination of transition metal ions to the SBT ligand, which is further supported by the appearance of other bands between 645 and 515 cm^{-1}corresponding to the stretching of the M–O group.[23]

^{1}H NMR AND ^{13}C NMR SPECTRA

Figure 3 shows the ^{1}H NMR spectra of SBT and SBT-Zn(II). In the spectrum of SBT, two resonance signals at 8.59 and 11.56 ppm correspond to amide (CH_2−NH−) and phenolic (Ar−OH) groups, respectively. These peaks shifted downfield due to the intermolecular hydrogen bonding when compared to their original position. The protons of the aromatic ring in SBT showed multiple resonance signals between 6.85 and 7.43 ppm.[24] The singlet resonance signal corresponding to the –CHO group was observed at 9.93 ppm. The other signals found at 3.62, 3.34, 2.08, and 1.74 ppm indicate the presence of the –CH_2–CH_2– group belonging to the glutaraldehyde moiety.

TABLE I
Elemental Analysis of SBT and Its Polymer Metal Complexes

		Elemental Analysis				
Compound (color)	Yield (%)	Carbon	Hydrogen	Nitrogen	Sulfur	Metal
SBT (light yellow)	74	70.21 (70.30)	6.61 (6.62)	6.33 (6.35)	7.81 (7.85)	-
SBT-Co(II) (pink)	76	63.07 (63.05)	6.84 (6.86)	6.13 (6.17)	7.02 (7.04)	6.45 (7.22)
SBT-Ni(II) (light green)	75	63.09 (63.12)	6.84 (6.88)	6.13 (6.10)	7.02 (7.08)	6.42 (6.40)
SBT-Cu(II) (blue)	74	65.31 (65.34)	6.62 (6.63)	6.35 (6.38)	7.27 (7.24)	7.20 (7.31)
SBT-Zn(II) (light yellow)	72	65.18 (65.15)	6.61 (6.64)	6.33 (6.36)	7.25 (7.28)	7.39 (7.40)

The calculated and (found) values.

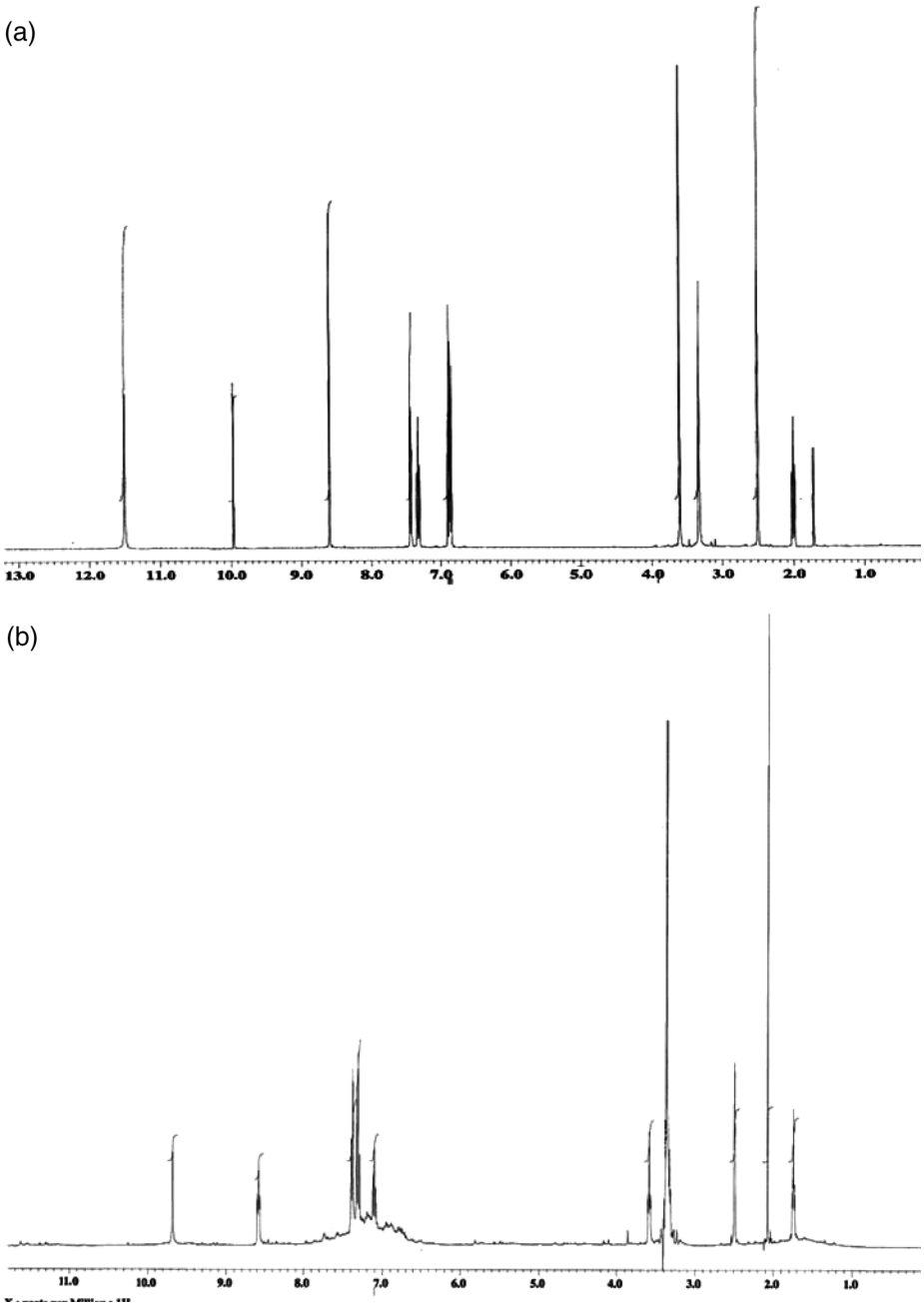

FIGURE 3. (a) ^{1}H-NMR spectra of polymeric ligand (SBT) (b) ^{1}H-NMR spectra of polymer metal complex [SBT-Zn(II)].

In the ^{1}H NMR spectrum of SBT-Zn(II), the resonance signal belonging to the –OH group was not detected due to the coordination of metal ions to the –OH group and due to the formation of O–M bonds. However, the resonance signal at 9.67 ppm belonging to the aldehyde (–CHO) group shifted toward downfield due to the coordination of metal ions.[25] The resonance signal of protons of the aromatic ring supports the intermolecular interaction between π-electron and the metal ions which become broader.[26]

The ^{13}C NMR resonance signals of SBT and SBT-Zn(II) at 19.56, 23.98,27.40, and 54.66 ppm are attributed to methylene groups (CH_2). The resonance signals around 161.86 and 179.92 ppm are assigned to thionyl and carbonyl carbon, respectively. The coordination of metal ions with the carbonyl group also supports the downfield shift of carbonyl resonance signal. Figure 4 shows the resonance signals of carbons in the aromatic ring in different environments at 115.71, 119.95, 121.94, 130.35, and 137.86 ppm. The ^{1}H NMR and ^{13}C NMR spectra of SBT and SBT-M(II) were recorded using DMSO as the solvent, which has the tendency to coordinate with the transition metal ions. But in this study, there was no coordinating effect of DMSO in the spectra of SBT and SBT-Zn(II).

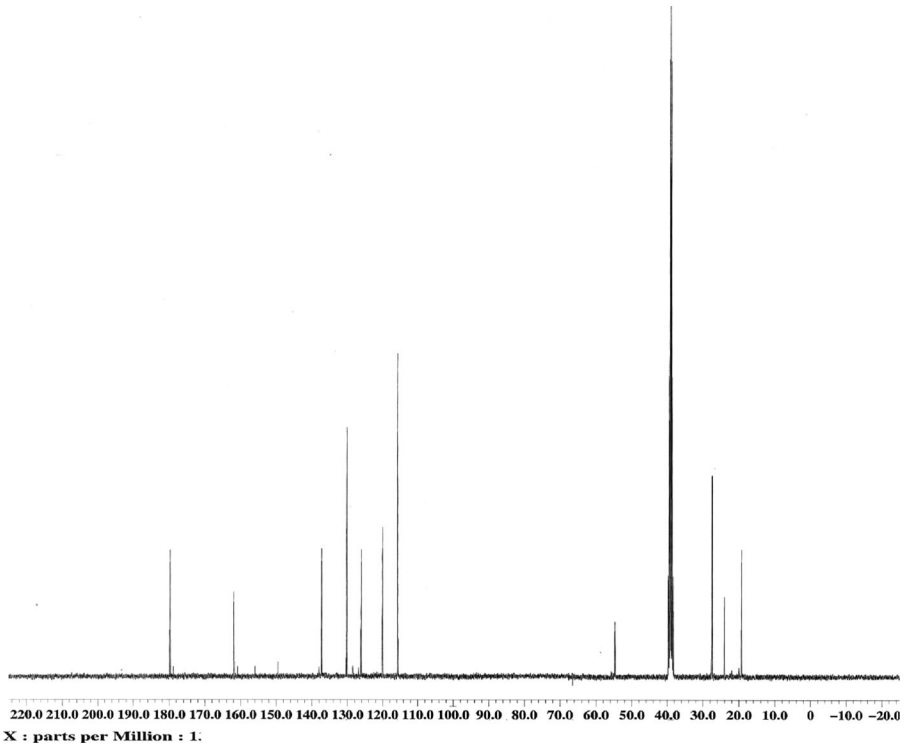

FIGURE 4. ^{13}C-NMR spectra of polymeric ligand (SBT).

MAGNETIC MOMENTS AND ELECTRONIC SPECTRA

Table II summarizes the electronic spectral parameters such as crystal field stabilization energy (10Dq), Racah parameter (B), nephelauxetic effect (β), the covalency parameter (β^0) values, and the magnetic moment value. DMSO was used as the solvent to determine the UV–visible spectra of SBT-M(II). The magnetic moment of SBT-Co(II) was found to be 4.64 BM corresponding to four unpaired electrons (4.90 BM) that suggests an octahedral geometry of Co(II). The magnetic moment of SBT-Co(II) was lower than the expected magnetic moment for free Co(II) ions. This lowering in the magnetic moment could be due to the polymeric nature of the complexes.[27] The UV–visible spectra of SBT-Co(II) show three adsorption bands at 14,842, 18,246, and 23,380 cm^{-1} corresponding to $^4T_{1g}(F) \rightarrow {}^4T_{2g}$, $^4T_{1g}(F) \rightarrow {}^4A_{2g}$ (F), and $^4T_{1g}(F) \rightarrow {}^4T_{1g}(P)$ transitions, respectively. The parameters, namely, 10Dq, B, β, and β^0 were found to be 11,224 cm^{-1}, 786 cm^{-1}, 0.84, and 16%, respectively. The value of magnetic moment for SBT-Ni(II) was 2.82 BM due to two unpaired electrons and indicating a spin free octahedral configuration. Lowering in the value of magnetic moment may be due to an antiferromagnetic effect, the influence of spin–orbital coupling in the ground state for spin doublet species,[28] or suggest the formation of dimeric or polymeric structures. In the electronic spectra of SBT-Ni(II), three electronic peaks were observed at 13,784; 16,328; and 23,846 cm^{-1}, which correspond to $^3A_{2g}(F) \rightarrow {}^3T_{2g}(F)$, $^3A_{2g}(F) \rightarrow {}^3T_{1g}(F)$ and $^3A_{2g}(F) \rightarrow {}^3T_{1g}(P)$ transition, respectively. The electronic spectral parameters 10Dq, B, and β were found to be 8,942 cm^{-1}, 878 cm^{-1}, and 0.80, respectively, and the β^0 value was 20%. The Racah parameter for free Ni(II) ions was found to be 1,080 cm^{-1}, whereas for SBT-Ni(II) it was found to be 878 cm^{-1} indicating the covalent nature of the SBT-M(II).[29] SBT-Co(II) and

TABLE II
Magnetic Moment and Electronic Spectral Data of Polymer Metal Complexes

			Electronic Spectral Data					
Compound	Magnetic Moment in BM[a]	ESR $g^{\|\|}/g^{\perp}$	Electronic transition (cm^{-1})	Assignment	10Dq (cm^{-1})	B (cm^{-1})	B	β^0 (%)
SBT-Co(II)	4.64	–	20,380	$^4T_{1g}(P) \leftarrow {}^4T_{1g}$ (F)	11,224	786	0.84	16
			18,246	$^4A_{2g}(F) \leftarrow {}^4T_{1g}(F)$				
			14,842	$^4T_{2g}(F) \leftarrow {}^4T_{1g}(F)$				
SBT-Ni(II)	2.82	–	23,846	$^3T_{1g}(P) \leftarrow {}^2A_{2g}(F)$	8,942	878	0.80	20
			16,340	$^3T_{1g}(F) \leftarrow {}^3A_{2g}(F)$				
			13,782	$^3T_{2g}(F) \leftarrow {}^3A_{2g}(F)$				
SBT-Cu(II)	2.04	2.540/ 2.098	24,620	Charge -transfer				
			16,340	$^2A_{1g} \leftarrow {}^2B_{1g}$				

[a]BM: Bohr magneton.

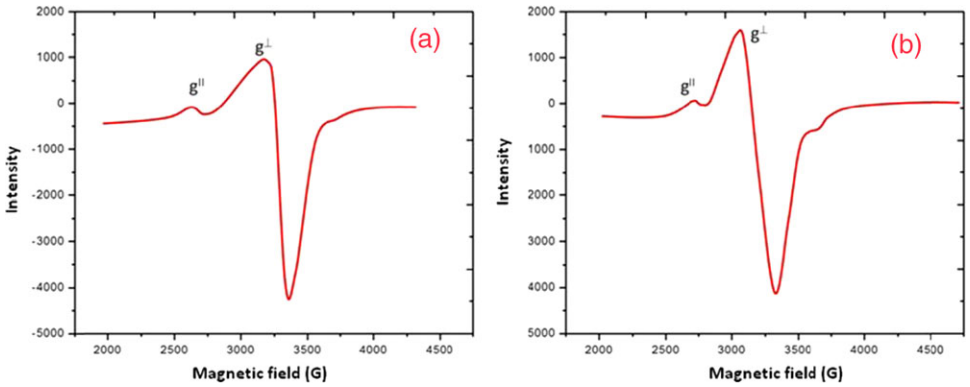

FIGURE 5. ESR spectra of SBT-Cu(II) (a) at 300K (b) at 77.

SBT-Ni(II) complexes showed an octahedral geometry because of the Co(II) and Ni(II) ions that coordinated with two water molecules.

The magnetic moment value for SBT-Cu(II) was found to be 2.04 BM due to the presence of one unpaired electron. The electronic spectra of SBT-Cu(II) showed two d–d transition bands at 16,340 to 24,620 cm^{-1} corresponding to $^2A_{1g} \leftarrow 2B_{1g}$ and charge-transfer spectra, respectively, due to the square–planar geometry around the Cu(II) ion.[30] In case of SBT-Zn(II), no electronic spectral peaks were observed= and the magnetic moment supports the diamagnetic nature of SBT-Zn(II).

ESR SPECTRA OF SBT-Cu(II)

Figure 5 illustrates the ESR spectrum of SBT-Cu(II). The spectrum at 77 K was almost identical to that at room temperature, which indicates that the geometry of Cu(II) did not change after lowering the temperature. The value of g^{II} and $g^{\perp}$ were found to be 2.536 and 2.094; the value of g^{II} was higher than that of $g^{\perp}$. This suggests that $d_{x^2-y^2}$ was ground state of Cu(II) ions, which is characteristic of a square–planar geometry. [31] The g^{II} value was lower than 2.3 that confirm the ionic character of the metal–ligand bond in the SBT-M(II), which agree with the observation of Kivelson and Neiman. The axial symmetry parameter G was used to find out the nature of ligands (weak field or strong field) and was calculated using g^{II} and g using the following equation:

$$G = \left(g^{II} - 2.002\right)/\left(g^{\perp} - 2.002\right)$$

If the axial symmetry parameter G is higher than 4.0, it indicates that the local axes are aligned in parallel or slightly misaligned and form a weak field ligand. If G is lower than 4.0, it indicates that significant exchange coupling is present and that the misalignment is appreciable and support the strong filed ligand. The observed value for the exchange interaction parameter for the SBT-Cu(II) was $G = 5.80$, suggesting that the ligand has a weak field.[32,33]

THERMOGRAVIMETRIC ANALYSIS

Figures 6–8 illustrate the thermograms of SBT and SBT-M(II), and Table III summarizes the thermal behavior of SBT and SBT-M(II) in the presence of nitrogen gas. The initial weight loss (1–2%) was observed in the temperature range 25–100°C for SBT and SBT-M(II), which was because of the weight loss of bonded moisture and trapped solvents. The thermal degradation of SBT can be divided into three stages: in the first stage, 24.41% weight

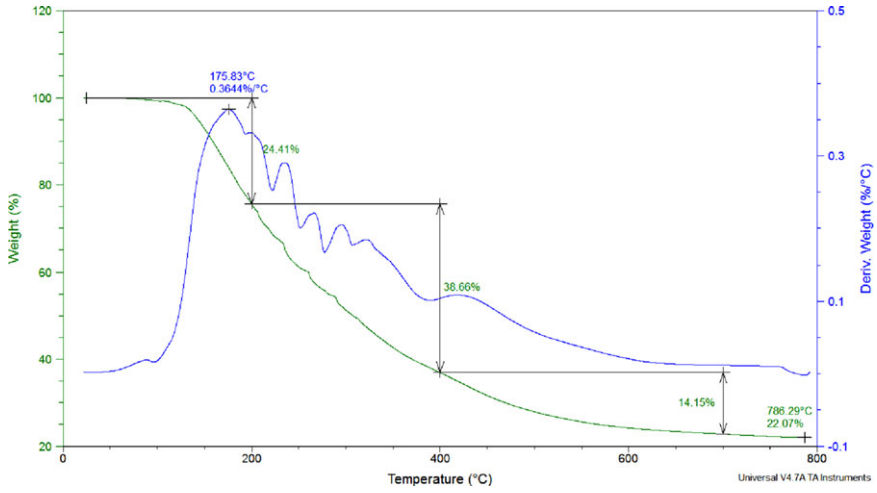

FIGURE 6. TGA/DTA thermograms of SBT.

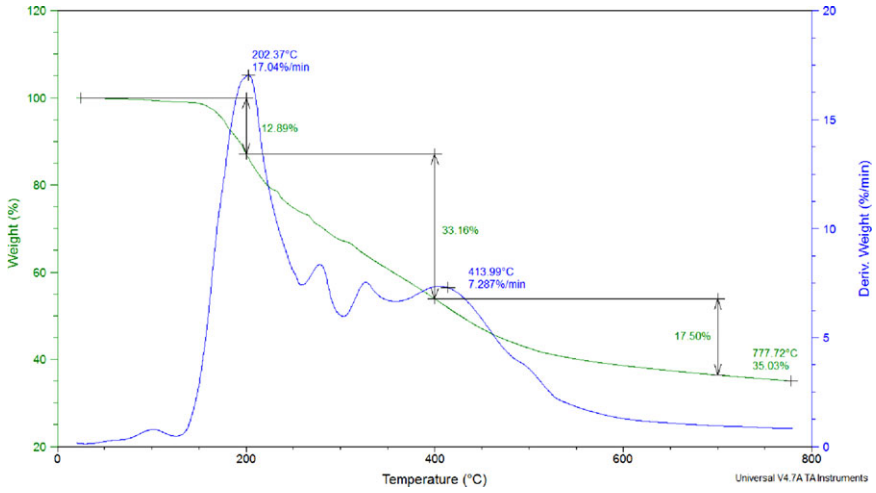

FIGURE 7. TGA/DTA thermograms of SBT-Co(II).

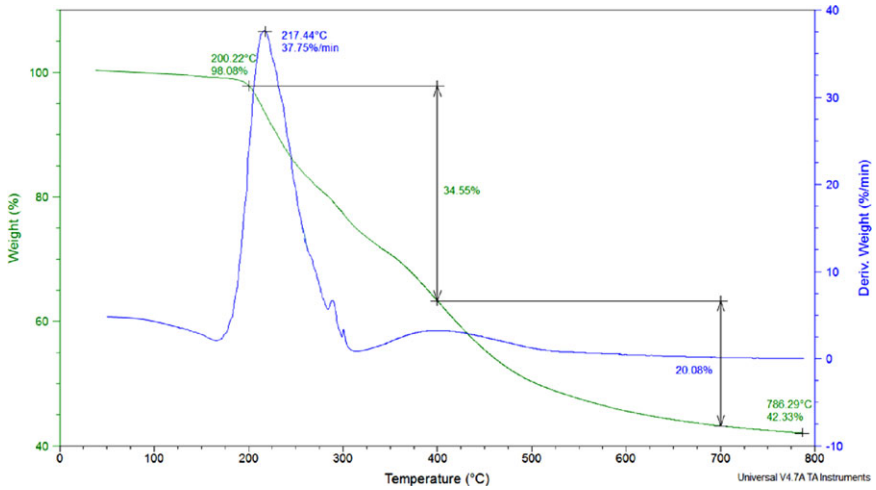

FIGURE 8. TGA/DTA thermograms of SBT-Cu(II).

(wt%) loss was observed between 155 and 200°C. The second stage was a fast thermal degradation stage with 38.66 wt% loss was observed from 200 to 400°C. The last stage is the cracking of the polymer in which 14.15 wt% of the total weight loss occurs up to786.29°C. However, in case of SBT-Co(II) and SBT-Ni(II), the initial weight loss was observed up to 200°C, which supports the removal of the metal-coordinated water molecules.[34] However, in case of SBT-Cu(II) and SBT-Zn(II), the initial weight loss was not due to the presence of coordinated water molecules. After the initial decomposition, the weight loss gradually increases to 50–55% up to 700°C.

TGA results reveal that the SBT-M(II) show higher thermal stability than that of the parental terpolymeric ligand (SBT). This is because after the coordination of metal ions, the percentage increase in the molecular weight and cross-linking of terpolymers and inorganic moieties takes place. The thermal stability of the prepared compounds was in the following order: SBT-Cu(II) > SBT-Co(II) > SBT-Ni(II) > SBT-Zn(II) > SBT-ligand, which supports the William Irriving equation.[35]

The results of thermal analysis in the second degradation step between 200 and 400 °C were used to find out the kinetic parameters of SBT and SBT-M(II)

TABLE III
Thermal Kinetic Parameters and Residue Weight at 750°C of Polymeric Ligand and Its Polymer Metal Complexes

Compound	Percentage Weight at 200°C	Activation Energy (KJ mol^{-1})	Preexponential Factor	R^2	Percentage Weight at 750°C
SBT	24.41	200	4.36E+00	0.930	23.06
SBT-Co(II)	12.89	193	4.52E+01	0.960	30.56
SBT-Ni(II)	12.86	186	4.56 E+02	0.970	30.89
SBT-Cu(II)	1.92	184	4.32E+00	0.975	40.50
SBT-Zn(II)	2.01	187	4.28E+01	0.960	38.92

Arrhenius theory was used to calculate the kinetic analysis during the thermal degradation of SBT and SBT-M(II) and also to support the first order reaction.[36]

$$k = A_{\exp}\left(-\frac{E}{RT}\right) \quad (1)$$

where k, RT, E, and A are constants of reaction rate, thermodynamic temperature (K), universal gas constant (R = 8.314 J mol^{-1}K^{-1}), activation energy, and preexponential factor respectively. The rate of thermal degradation of SBT and SBT-M(II) can be represented as given below:

$$\frac{d\alpha}{dt} = k(1-x) \quad (2)$$

where α is the weight loss fraction and is calculated according to the equation given below:

$$\alpha = \frac{m_0 - m_t}{m_0 - m_f}$$

where m_0, m_t, and m_f are the initial mass at 200°C, mass at a time during thermal degradation, and final mass of SBT and SBT-M(II) at 400°C. When the thermal degradation is carried out at different heating rates, the heating rate constant (β) can be represented with the function of time as given below:

$$T = \beta t + T_0 \quad (3)$$

After differentiating of Eq. (3):

$$dT = \beta dt$$

The thermal degradation rate in Eq. (2) can now be represented as below:

$$\frac{d\alpha}{1-\alpha} = \frac{k}{\beta}\,dT \quad (4)$$

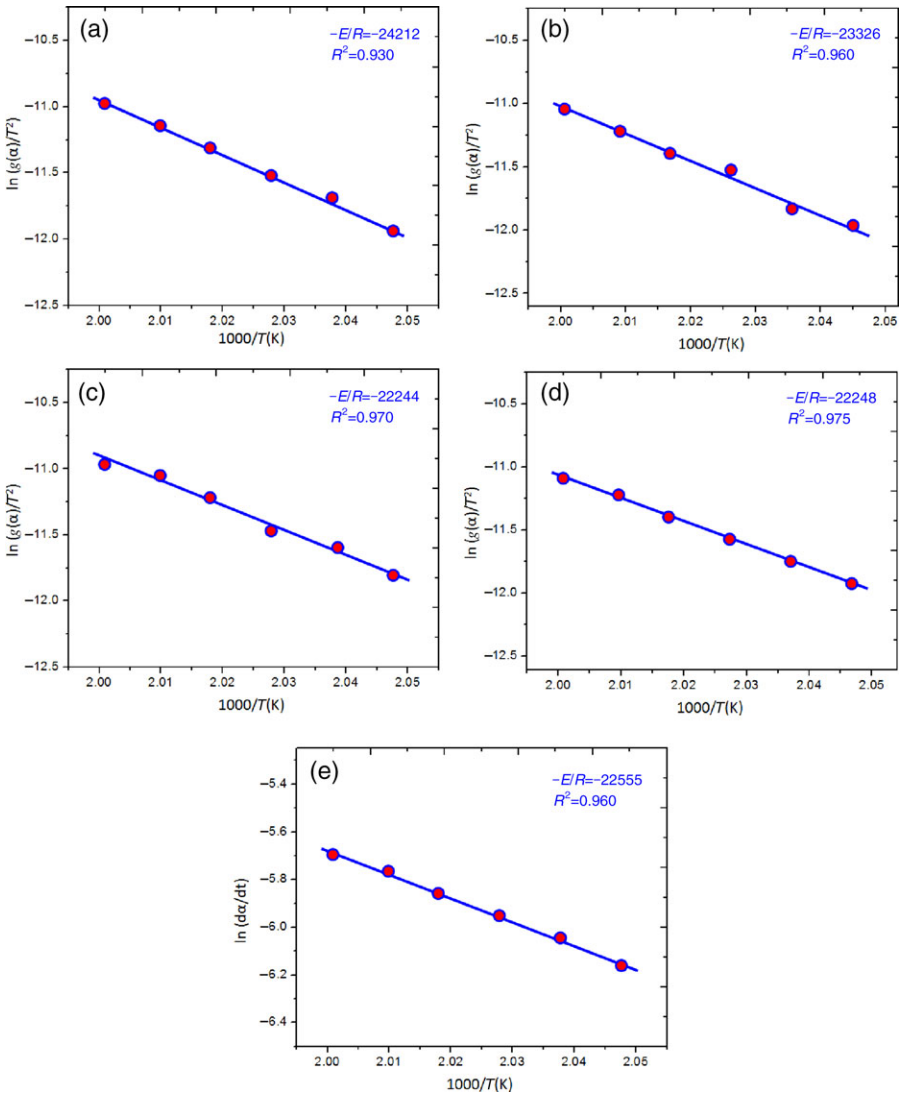

FIGURE 9. Thermal kinetiks plot of polymeric ligand (SBT) and polymer metal complexes.

TABLE IV
Antibacterial Activity of SBT and Its SBT-M(II)

Compound	Zone of Inhibition[a] (mm) 50 μg/disk				
	Staphylococcus aureus	*Salmonella typhi*	*B. subtilis*	*E. coli*	*P. aeruginosa*
SBT	14	15	12	17	17
SBT-Co(II)	17	17	19	17	19
SBT-Ni(II)	20	17	17	17	19
SBT-Cu(II)	21	20	20	20	22
SBT-Zn(II)	19	17	19	21	20
Kanamycin[b]	29	29	27	29	30
DMSO[c]	–	–	–	–	–

[a]18–30 mm = significantly active; 10–17 mm moderately active; <10 mm = weakly active.
[b]Standard drug (positive control).
[c]Solvent (negative control).

TABLE V
Antifungal Activity of SBT and Its SBT-M(II)

Compound	Zone of Inhibition[a] (mm) 100 μg/disk				
	C. albicans	*M. indicus*	*A. flavus*	*A. niger*	*F. solani*
SBT	13	14	14	16	16
SBT-Co(II)	16	18	19	17	18
SBT-Ni(II)	18	16	18	16	17
SBT-Cu(II)	20	19	19	21	20
SBT-Zn(II)	17	18	17	18	19
Miconazole[b]	22	25	25	25	25
DMSO[c]	–	–	–	–	–

[a]18–30 mm = significantly active; 10–17 mm moderately active; <10 mm = weakly active.
[b]Standard drug (positive control).
[c]Solvent (negative control).

After integration function of Eq. (4), we get

$$g(\alpha) = \int_0^{\alpha} \frac{\mathrm{d}a}{\mathrm{d}t} = \frac{A}{\beta} \int_0^{t} \exp(-E/RT)\mathrm{d}T \tag{5}$$

where $g(\alpha) = -\ln(1-\alpha)$.

Equation (5) is integrated by using the Coats–Redfern method as given below:

$$\ln(g(\alpha))/T^2 = \ln(AR/\beta E[1-2RT/E]) - E/RT \tag{6}$$

where $g(\alpha)$ is the kinetic mechanism function in integral form.

As the term of $2RT/E$ can be neglected, because this value is much less than 1, Equation (6) can be represented as

$$\ln \frac{g(\alpha)}{T^2} = \ln\left(\frac{AR}{\beta E}\right) - \frac{E}{R}\frac{1}{T} \tag{7}$$

A linear plot between $\ln(g(\alpha)/T^2)$ varies with $1/T$ representing the slope $(-E/R)$. However, the preexponential factor A can be calculated using intercept of the linear plot with the y axis. The activation energy (E) and preexponential factor (A) of SBT and SBT-M(II) can be determined by the slope and intercept (Fig. 9). The results of thermal kinetics reveal that SBT-Cu(II) show higher E value than other terpolymer complexes.

BIOLOGICAL ASSAY

Table IV and V summarize the antimicrobial activities of SBT and SBT-M(II) against several bacteria and fungi. SBT showed inhibition zone of 12, 14, and 15 mm against *B. subtilis*, *Staphylococcus aureus*, and *Salmonella typhi,* respectively. However, SBT-Co(II) showed the inhibition zones of 19, 19, and 17 mm against *P. aeruginosa*, *B. subtilis*, and *Staphylococcus aureus*,, respectively. SBT-Ni(II) showed promising antibacterial activities against all the tested bacteria with a maximum zone of inhibition of 20 mm against *Staphylococcus aureus*. The SBT-Cu(II) showed higher antibacterial activities than other terpolymeric complexes when tested against *Staphylococcus aureus* and *P. aeruginosa* with 21 and 22 mm zone of inhibition, respectively. It was also observed that SBT-M(II) showed higher zone of inhibition than SBT owing to the coordination of transition metal ions. A standard drug, kanamycin (30 μg), was used as a standard drug to compare the antibacterial activities. The results revealed that the synthesized terpolymers were significantly active against all the tested bacteria in this study.

The antifungal activity of the SBT and SBT-M(II) was carried out according to previously reported methods, and the results are presented in Table V. When SBT was screened against *M. indicus*, *A. flavus*, and *A. niger* the zone of inhibition values were found to be 14, 14, and 16 mm, respectively. The SBT-Ni(II) showed inhibition zone values of 16, 16, and 18 mm against *C. albicans*, *A. niger*, and *M. indicus*, respectively, whereas SBT-Zn(II) showed the zone of inhibition of 19 and 18 mm against *F. solani*

and *M. indicus*, SBT-Cu(II) showed the highest zone of inhibition values with 19, 19, and 21 mm against *M. indicus*, *A. flavus*, and *A. niger*, respectively, when compared with other metal complexes. The results from this study reveal that after coordination of metal ions with terpolymeric ligand the antimicrobial activity increased which supports the Overtone's concept and Chelation theory. The coordination of metal ions reduced the polarity of the metal ions because of the decrease in the positive charge after coordination with donor atoms of ligands. However, coordination increases the delocalization of π-electrons in the chelating ring thereby enhancing the antimicrobial properties of the metal-coordinating compounds. The enhanced antimicrobial activity of SBT-M(II) was due to the penetration of SBT-M(II) into the lipid bilayer, thereby blocking the metal binding sites in the enzymes of the tested microorganisms. There are several other factors such as conductivity, solubility, and metal–ligand bond length that can affect the antimicrobial activity.[37–39]

CONCLUSION

A novel terpolymeric ligand (SBT) was prepared via the polycondensation reaction of salisaldehyde and phenylthiourea with formaldehyde, and its terpolymeric metal complexes [SBT-M(II)] were prepared with transition metal ions. The synthesized compounds were characterized using various analytical techniques, and the results revealed that SBT-Co(II) and SBT-Ni(II) have octahedral geometry due to the coordination of two metal ions. However, the SBT-Cu(II) and SBT-Zn(II) represent square–planar and tetrahedral geometry, respectively, due to four coordination number. All the synthesized compounds were screened for their antimicrobial activities which showed excellent results against the tested bacteria and fungi. The SBT-Cu(II) showed higher antimicrobial activity than corresponding terpolymeric metal complexes, and terpolymeric ligand due to higher thermal stability of Cu(II) ions. Overall, in this study, the synthesized compounds showed promising antimicrobial activities against several bacteria and fungi; therefore, they can be used in various medical and biomedical applications, and, in future, they can also be used as antimicrobial agents.

Acknowledgement

The authors extend their appreciation to the Deanship of Scientific Research at King Saud University for funding this work through research group no. PRG-1436-19.

References

1. Catanescu, O.; Grigoras, M.; Colotin, G.; Dobreanu, A.; Hurduc, N.; Simionescu, C. I. Eur Polym J 2001, 37, 2213.
2. Stevans, M. P. Polymer Chemistry, 2nd ed.; Oxford University Press: New York, 1990.
3. Venugaopala, K. N.; Jayashree, B. S. Indian J Heterocycl Chem 2003, 12, 307–310.
4. Vashi, K. O.; Naik, H. B.; Eur J Chem 2004, 1, 272–276.
5. Brzezińska, E.; Kośka, G. Walczyński, K. J., Chromatography A 2003, 1007, 145–155.
6. Rana, A.; Siddiqui, N.; Khan, S. A.; Haque, S. E.; Bhat, M. A. Eur J Med Chem 2008, 43, 1114–1122.
7. Alshehri, S. M.; Naushad, M.; Ahamad, T.; Alothman, Z. A.; Aldalbahi, A. Chem Eng J 2014, 254, 181–189.
8. Neelakantan, M. A.; Marriappan, S. S.; Dharmaraja, J.; Jeyakumar, T.; Muthukumaran, K. Spectrochim Acta, Part A 2008, 71, 628–635.
9. Alshehri, S. M.; Aldalbahi, A.; Ahamad, T. 2015, 34, 21512.
10. Mamdouh, S. M.; Azza, E. H. A.; Wael, M. A. J Molec Struc 2015, 1095, 135–143.
11. Nishat, N.; Ahmad, S.; Ddin, R.; Ahamad, T. J Appl Polym Sci 2006, 100, 928.
12. Ahamad, T.; Kumar, V.; Nishat, N. Polym Int 2006, 55, 1398–1406.
13. Nishat, N.; Ahamad, T.; Alshehri, S. M.; Parveen, S. Eur J Med Chem 2010, 45, 1287.
14. Ahamad, T.; Alshehri, S. M. Spectrochim Acta Part A, 2013, 108, 26–31.
15. Alshehri, S. M.; Ahamad, T.; Aldalbahi, A.; Alhokbany, N. Adv Polym Technol 2016, 35, 21528.
16. Nishat, N.; Rasool, R.; Khan, S. A.; Parveen, S. J Coord Chem 2011, 64, 4054.
17. Ahamad, T.; Alshehri, S. M. Adv Polym Technol 2013, 32, 21350.
18. Ahamed, M. A. R.; Burkanudeen, A. R. Adv Polym Technol, 2013, 32, 21376.
19. Ahamad, T.; Kumar, V.; Nishat, N. J Biomed Mater Res A 2009, 88, 288.
20. Nishat , N.; Ahamad, T.; Ahmad, S.; Parveen, S, J Coord Chem 2011, 64, 2639.
21. Hasnain, S.; Zulfequar, M.; Nishat, N. Polym Adv Technol 2012, 23, 1002–1010..
22. Freedman, H. H. J Am Chem Soc 1961, 83, 2900.
23. Manimaran, A.; Prabhakaran, R.; Deepa, T.; Natarajan, K.; Jayabalakrishnan, C. Appl Org Chem 2008, 22, 353.
24. Esref, T.; Mehmet, A.; Mehmetand, G. U. J Coord Chem 2004, 57, 583–589.
25. Raja, S. Aa.; Subhaa, R.; Jeyakumarb, D.; Abdul, R. B. Separation Purif Technol 2013, 116, 366–377.
26. Salimon, J.; Salih, N.; Hussien, H.; Yousif, E. Eur J Sci Res 2009, 31, 256–264.
27. Rathore, K.; Rajiv, K. R.; Singh, H. B. Eur J Chem 2010, 566–572.
28. Hasnain, S.; Nishat, N. Spectrochim Acta, Part A 2012, 95, 452–457.
29. Nishat, N.; Ahamad, T.; Zulfequar, M.; Hasnain, S. Appl Polym Sci 2008, 110, 305–3312.
30. Nishat, N; Ahamad, T. J Appl Polym Sci 2008, 107, 2280.
31. Kivelson, D.; Neiman, R. J Chem Phys 1985, 35, 149.
32. Narang, K.; Singh, V. Trans Met Chem 1996, 21, 5079.
33. Rasool, R.; Hasnain, S. Spectrochim Acta, Part A 2015, 148, 435–443.
34. Rasool, R.; Hasnain, S.; Nishat, N. J Inorg Organomet Polym Mater 2015, 25, 763–271.
35. Irving, H.; Williams, H. J Chem Soc 1993, 3192.
36. Pan, H.; Shupe, T. F.; Hse, C. Y. J Appl Polym Sci 2002, 108, 1837–1844.
37. Chohan, Z.; Munawar, A.; Supuran, C. Met Based Drugs 2011, 8, 137–143.
38. Iqbal, J.; Tirmizi, S. A.; Wattoo, F. H.; Imran, M. Turk J Biol 2006, 30, 1–4.
39. Hanan, F. A. E.; Gehad, G. M. J Molec Struc 2016, 104, 91–95.